Using Active Load-Pull with Modulated Signals to Optimize Power and Linearity

Xenofon Konstantinou[1], John D. Albrecht[2], and John Papapolymerou[3]
Department of Electrical & Computer Engineering, Michigan State University, East Lansing, MI 48824, USA
{[1]konstan8, [2]jalbrech, [3]jpapapol}@egr.msu.edu

***Abstract*—Active Load-Pull (L-P) measurements using modulated signals are performed on a packaged GaN HEMT to optimize power and linearity. The measurements are taken using single-tone (1-tone), two-tone (2-tone), and modulated (128-QAM) signals at 2 GHz. A test fixture with a 6 W commercial GaN HEMT is used as the device-under-test (DUT). Linearity is optimized by minimizing IM3 and ACPR. Furthermore, a comparison of the optimized load power (P_L) performance between 1-tone and 128-QAM is made. Our results show that the impedance matching conditions that optimize either power or linearity can be reliably predicted via active L-P using modulated signals. We also find that there are considerable differences between 1-tone and the modulated signals in the P_L contours and optimal P_L impedance matching conditions. These ascertainments could impact power amplifier design depending on the power and linearity specification trade-offs.**

***Index Terms*—5G, active load-pull, GaN, HEMT, linearity, modulation, power amplifier.**

I. Introduction

L-P characterization is a powerful tool used extensively as a large-signal measurement technique to characterize transistors, power amplifiers (PAs), and other RF components, originally aiming to find the optimum matching conditions at the fundamental frequency f_0 to maximize gain or output power [1]. With the rise of complex modulated waveforms in modern mobile networks and wireless applications, there is strong interest in adapting L-P techniques to additionally optimize the linearity of PAs for 5G communication frequency bands. The Third-Order Intermodulation (IM3) and the Adjacent-Channel Power Ratio (ACPR) are key parameters of interest [2]. Considering the high Peak-to-Average Power Ratio (PAPR) signals used in contemporary mobile networks, developing L-P measurement techniques for modulated signals is potentially very powerful, analogous to high output power optimization.

To date, the majority of L-P techniques utilize passive harmonic L-P systems due to their comparatively simple system control software demands and high-power handling. Nonetheless, they suffer from losses in harmonic tuners, cables, and probes, which limit the magnitude of the reflection coefficient (Γ) the system can present and narrow the range of characterization conditions, thus making some Smith Chart impedances impossible to present to the DUT input/output. Further, the electrical delay results in high phase changes that restrict the abilities of the system when handling wideband modulated signals. In contrast, active L-P systems use amplifiers and can overcome the aforementioned restrictions (losses and bandwidth) [3]. Their ability to present the DUT with any impedance, handle wideband modulated signals, and significantly increase measurement speed makes them a potential candidate to help design PAs that will satisfy the power, efficiency, and linearity requirements in future 5G applications.

Thus far, results from linearity characterization using passive L-P [2], [4], [5], as well as 1-tone active L-P for power optimization [6], have been published in the literature. Nonetheless, the need for techniques to optimize the trade-off between power and linearity in PA design for 5G networks entails the incorporation of both power and linearity measurements with modulated signals in a single active L-P technique. In this work, for the first time to the best of our knowledge, active L-P with modulated signals is used on a GaN HEMT to optimize power and linearity. The measurements are taken at 2 GHz using the Maury Microwave MT2000 Mixed-Signal Active L-P System. We use 1-tone, 2-tone, and 128-QAM signals. L-P contours are presented for P_L, as well as for IM3 and ACPR. Moreover, a comparison is made between 1-tone and 128-QAM in order to identify the differences of the two signals in the matching conditions that optimize P_L. GaN is chosen as the test vehicle given its presence in existing wireless transmitter applications (e.g., base station transmitters) and its strong candidacy for high-efficiency power amplifiers in 5G networks. In addition, GaN HEMT amplifiers are applicable to high-power broadband PAs for radar transmitters and receivers across the spectrum [7]–[10].

II. HEMT Test Fixture Design and Fabrication

Given the additional complications of on-wafer probe testing at 5G [13], we focus on a packaged transistor to isolate the effects of modulated waveforms from other testing complexities. The design parameters of the test fixture illustrated in Fig. 2 are summarized in Table I. An R-C network is used at the gate of the GaN HEMT (T_1) to provide stability. All component values are chosen to optimize the trade-off between unconditional stability and power gain. In order to maintain a safe T_1 temperature and avoid self-heating effects that would lead to an input reflection coefficient shift and dynamic input mismatch, an aluminum heat sink is used. T_1 is soldered onto a copper sheet that is thereupon attached to the heat sink.

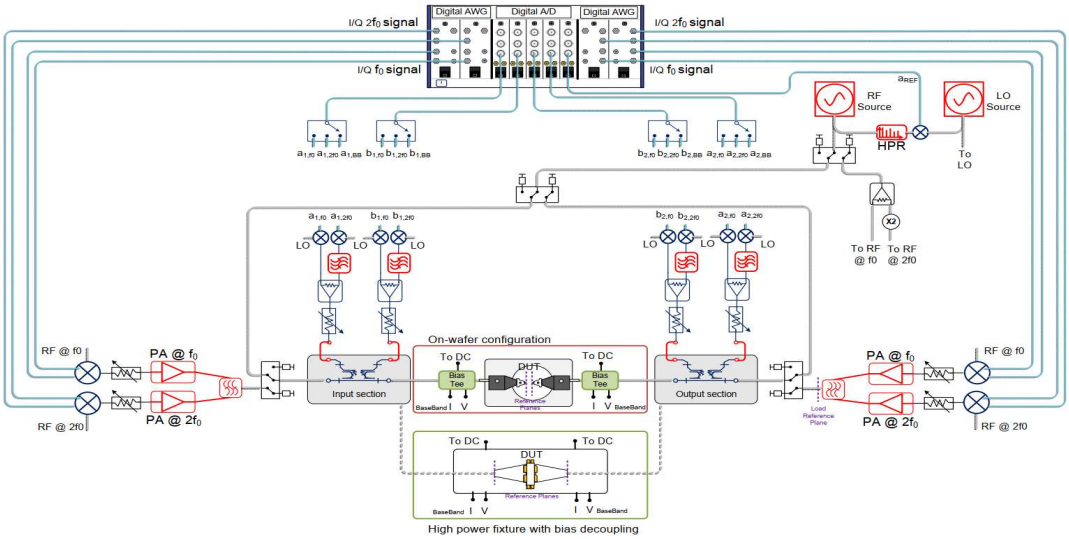

Fig. 1: Simplified block diagram of the MT2000 Mixed-Signal Active L-P System [11], [12]. In this configuration example, external amplifiers are used both on the source and load side (DUT input and output, respectively) to tune Γ at f_0 and $2f_0$. In our work, measurements are taken only at f_0, hence only one amplifier is used per side.

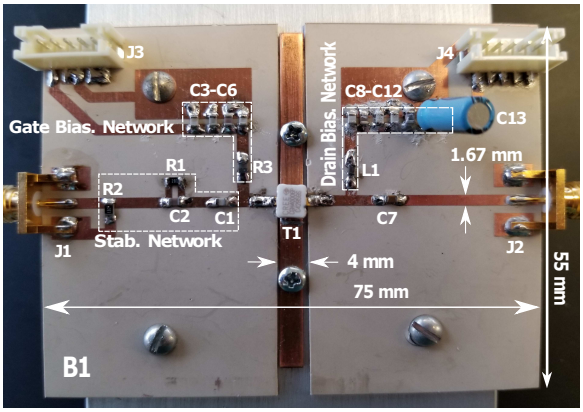

Fig. 2: The in-house fabricated GaN HEMT test fixture (DUT).

TABLE I: Summary of the test fixture design parameters.

Ref.	Corresponding Values/Parameters/Description
T_1	CREE CGH40006P
B_1	RT/duroid 6035HTC, 0.032", 35 µm copper cladding
C_1, C_2, C_7	1.3 pF, 6 pF, 330 pF
C_3-C_6	330 pF, 450 pF, 1 µF, 10 µF
C_8-C_{12}	100 pF, 330 pF, 450 pF, 1 µF, 10 µF
C_{13}	33 µF
R_1, R_2, R_3	200 Ω, 300 Ω, 50 Ω
L_1	2.2 µH
J_1, J_2	CONN SMA EDGE MNT
J_3, J_4	CONN HEADER SMD

III. Measurements and Discussion

A. Measurement Setup Description

The MT2000, illustrated in Fig. 1, uses an open-loop architecture to tune Γ_x, where $x = \{S, L\}$, on the source and load side (at the DUT input and output, respectively), by directly injecting arbitrary signals into the DUT. Γ_x represents the ratio of power waves, b_x/a_x, with a_x being the incident and b_x being the DUT-generated power wave, respectively. The a_x- and b_x-waves, and thereby Γ_x, are controlled via software iterations. When the DUT is excited with a modulated signal a_S, it generates signals b_S and b_L. By measuring all a_x- and b_x-waves, the system estimates the waves that need to be injected to the DUT at each iteration to achieve the desired Γ_S and Γ_L. The injected a_x-waves are generated by wideband baseband arbitrary waveform generators (AWG) and up-converted using in-phase/quadrature (I/Q) modulators. The acquired DUT-generated signals are down-converted to an IF frequency and then sampled with wideband A/D converters [3], [12].

B. Measurement Approach

The measurements are conducted using 1-tone, 2-tone, and 128-QAM continuous-wave (CW) signals at $f_0 = 2$ GHz. Different levels of available source power (P_{avs}) are applied to investigate the differences in P_L, IM3, and ACPR contours with respect to a changing drive. Every contour line encloses load impedance (Z_L) points that correspond to a specific attained parameter (P_L/IM3/ACPR) value, or better (larger in absolute value). The optimal Z_L for the corresponding parameter is located at the center of each contour family and is indicated by P_i on the Smith Chart. For IM3 and ACPR, the measurements are performed in two adjacent frequency channels below and above the signal bandwidth. IM3 and ACPR are measured using a 2-tone and a 128-QAM input signal, respectively. The 2-tone signal is chosen to have a tone spacing of 50 MHz, while the 128-QAM signal is chosen with a PAPR of 7 dB, a symbol rate of 65 Msym/sec, a

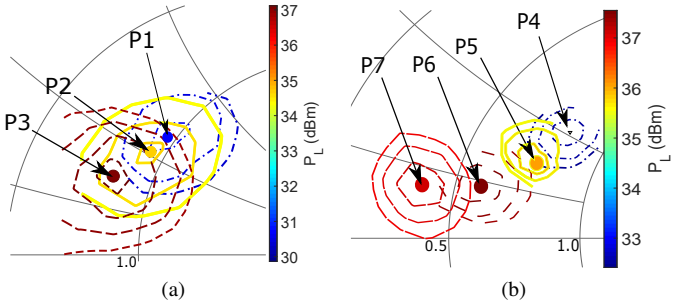

Fig. 3: P_L contours, with increasing P_{avs}, for the: (a) 1-tone signal, (b) 128-QAM signal. Every contour family, indicated by a different line type, corresponds to a different P_{avs} level.

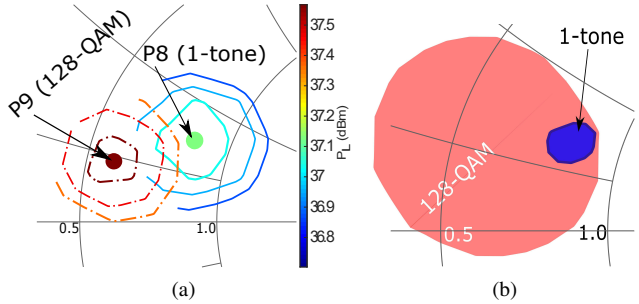

Fig. 4: P_L comparison of 1-tone and 128-QAM for a constant $P_{avs} = 28$ dBm: (a) P_L contours, with every contour family, indicated by a different line type, corresponding to a different signal waveform, (b) isolated contours for $P_L \simeq 37$ dBm.

roll-off factor of 0.22, square root raised-cosine pulses, and a bandwidth of 80 MHz.

An SOLT calibration is performed to bring the reference planes to the inputs of J_1 and J_2. In order to accurately measure IM3 and ACPR, the MT2000 source signal pre-distortion feature is used to reduce the distortion of the actual source signal with respect to the ideal source signal by extracting the distortion caused by the two external amplifiers. T_1 is biased with $V_{GS} = -2.74$ V and $V_{DS} = 28$ V, maintaining $I_{DS} = 100$ mA and $I_{GS} = 0$ [14]. To locate the 1 dB compression point (P_{1dB}), a 1-tone P_{avs} sweep is performed, showing that P_{1dB} occurs for $P_{avs} = 32$ dBm. The 128-QAM signal has a PAPR of 7 dB, which needs to be taken into account during the L-P measurements. While the 128-QAM signal gets amplified as P_{avs} approaches P_{1dB}, T_1 is driven to saturation, causing the gain and P_L of the DUT to be confined due to nonlinearity. Hence, to ensure a fair comparison between 1-tone and 128-QAM signal amplifications, a careful choice of P_{avs} has to be made to exhibit high-power operation while avoiding nonlinearity. In our comparison, we let P_{avs} = 28 dBm. Finally, for all L-P measurements, the source impedance, Z_S, is set to 50 Ω, thus there is mismatch and a considerable reflection at the input and the power at the T_1 input is lower than P_{avs}.

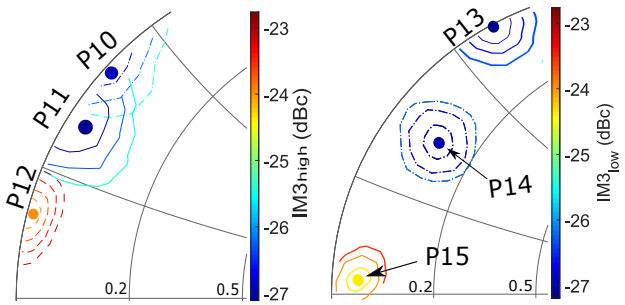

Fig. 5: IM3 contours, with increasing P_{avs}, for: (a) $IM3_{high}$, (b) $IM3_{low}$.

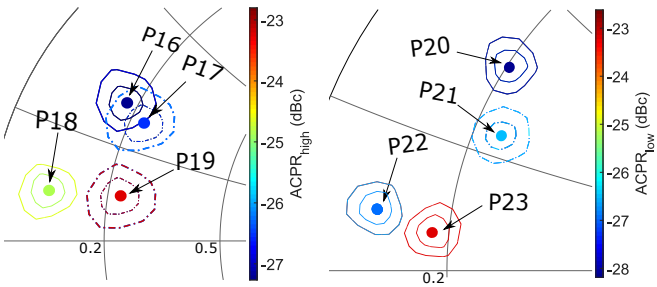

Fig. 6: ACPR contours, with increasing P_{avs}, for: (a) $ACPR_{high}$, (b) $ACPR_{low}$.

C. P_L Active L-P Measurements

The measurements for all optimal load impedances are summarized in Table II. The P_L contours for 1-tone and 128-QAM are shown in Fig. 3, with a peak P_L of 37.2 and 37.7 dBm attained, respectively, for P_{avs} = 28 dBm. The effects of nonlinearity on high-PAPR signals near the saturation region can be seen on the 128-QAM contours, since increasing P_{avs} from 28 to 32 dBm results in a decreased P_L.

Furthermore, a comparison of 1-tone and 128-QAM P_L performance for P_{avs} = 28 dBm is illustrated in Fig. 4a. Maximum P_L for the two signals is acquired for different Z_L, with 128-QAM providing a higher P_L. This means that if the DUT output is matched to P_8 based on the 1-tone contours, a 128-QAM operation would give P_L = 37.2 dBm $\simeq$ 5.3 W, whereas the maximum attainable is 37.7 dBm $\simeq$ 5.9 W. The difference is 0.6 W, which can be a significant power value in wireless communications. Another way to underline this difference is to isolate the contours for a certain P_L level, as shown in Fig. 4b. The 1-tone contour for $P_L \simeq 37$ dBm overlaps with the corresponding 128-QAM contour only over a very small region of the latter.

D. Linearity Active Load-Pull Measurements

For linearity, 2-tone IM3 and 128-QAM ACPR measurements are performed in two adjacent frequency channels below and above the signal bandwidth. The

TABLE II: The L-P measurement results for all $P_{i\in[1,23]}$.

Figure	P_i	Signal Type	Z_L (Ω)	P_{avs} / P_L (dBm)	IM3 / ACPR (dBc)	Figure	P_i	Signal Type	Z_L (Ω)	P_{avs} / P_L (dBm)	IM3 / ACPR (dBc)
3a	P_1	1-tone	48.6 + j31.4	20 / 30.7	– / –	5b	P_{13}	2-tone	0.3 + j29.8	20 / –	-27.6 / –
	P_2	1-tone	47.4 + j26.7	24 / 34.4	– / –		P_{14}	2-tone	5.8 + j16.4	24 / –	-27.3 / –
	P_3	1-tone	40.9 + j16.7	28 / 37.2	– / –		P_{15}	2-tone	1.3 + j0.4	28 / –	-24.8 / –
3b	P_4	128-QAM	40.2 + j25.8	20 / 32.6	– / –	6a	P_{16}	128-QAM	8.8 + j14.7	20 / –	– / -27.5
	P_5	128-QAM	37.7 + j15.6	24 / 35.7	– / –		P_{17}	128-QAM	11.6 + j13.5	24 / –	– / -26.7
	P_6	128-QAM	29.1 + j9.1	28 / 37.7	– / –		P_{18}	128-QAM	4.6 + j4.2	28 / –	– / -25
	P_7	128-QAM	20.6 + j7.6	32 / 37.2	– / –		P_{19}	128-QAM	11.3 + j5	32 / –	– / -23.3
4a	P_8	1-tone	40.9 +j16.7	28 / 37.2	– / –	6b	P_{20}	128-QAM	10.2 + j17.8	20 / –	– / -28.4
	P_9	128-QAM	29.1 + j9.1	28 / 37.7	– / –		P_{21}	128-QAM	12.2 + j12	24 / –	– / -26.6
5a	P_{10}	2-tone	0.4 + j18.7	20 / –	-27 / –		P_{22}	128-QAM	4.6 + j4.2	28 / –	– / -27
	P_{11}	2-tone	1.6 + j14.3	24 / –	-25.7 / –		P_{23}	128-QAM	8.7 + j3	32 / –	– / -23.3
	P_{12}	2-tone	0.5 + j18.7	28 / –	-23 / –						

measurements, illustrated in Fig. 5 and Fig. 6, show IM3 and ACPR values for each P_{avs} level being similar. All optimal Z_L points are adjacent on the Smith Chart and move towards the real axis as P_{avs} level increases, with linearity worsening, as expected, since the drive moves closer to saturation.

IV. Conclusions

An active L-P technique with modulated signals is used to optimize power and linearity, utilizing a packaged GaN HEMT test fixture. P_L, IM3, and ACPR measurements are performed for different levels of P_{avs}. Then, a comparison of the P_L performance between a 1-tone and a 128-QAM signal is made. The technique demonstration shows that the matching conditions to optimize either power or linearity can be reliably predicted via active L-P using modulated signals. It is also concluded that there are considerable differences between 1-tone and modulated signals in the matching conditions that maximize P_L. Therefore, active L-P is a potentially powerful tool for designing PAs that can handle modulated waveforms and provides more capabilities than active L-P techniques limited to 1-tone signals. Comparing to passive L-P using modulated signals, active L-P provides the capability of much faster, accurate, and reliable measurements due to the transcendence of loss and bandwidth limitations. The drawback of active L-P, compared to passive, is the requirement for large external RF amplifiers to deliver the desired Γ, since the external amplifiers have to be able to handle more power that the DUT itself to ascertain the required power waves, and also the fact that active L-P systems are more expensive than passive ones.

Acknowledgment

The authors would like to thank Maury Microwave for supplying external amplifiers, S. Dudkiewicz and M. Marchetti for technical discussions, Y. He for assisting with the fixture fabrication, and Rogers Corp. for supplying the board laminate.

References

[1] S. Cripps, *RF Power Amplifiers for Wireless Communications*, ser. Artech House microwave library. Artech House, 2006.

[2] S. A. K. Kahil *et al.*, "Linearity characterization of GaN HEMT technologies through innovative on-wafer multi-tone load-pull measurements," in *2016 11th European Microwave Integrated Circuits Conference (EuMIC)*, Oct 2016, pp. 37–40.

[3] M. Marchetti *et al.*, "Active Harmonic Load–Pull With Realistic Wideband Communications Signals," *IEEE Trans. Microw. Theory Techn.*, vol. 56, no. 12, pp. 2979–2988, Dec 2008.

[4] J. X. Qiu *et al.*, "Linearity characterization and optimization of millimeter-wave gan hemts," *IEEE Transactions on Microwave Theory and Techniques*, vol. 59, no. 12, pp. 3419–3427, Dec 2011.

[5] M. Ubostad and M. Olavsbråten, "Analysis of an rf power amplifier for envelope tracking based on load-pull data," in *2009 74th ARFTG Microwave Measurement Conference*, Nov 2009, pp. 1–4.

[6] A. A. Nawaz *et al.*, "Harmonic tuning of stacked sige power amplifiers using active load pull," *IEEE Microw. Wireless Compon. Lett.*, vol. 28, no. 3, pp. 245–247, March 2018.

[7] U. K. Mishra *et al.*, "GaN-Based RF Power Devices and Amplifiers," *Proceedings of the IEEE*, vol. 96, no. 2, pp. 287–305, Feb 2008.

[8] U. K. Mishra, P. Parikh, and Y.-F. Wu, "AlGaN/GaN HEMTs-an overview of device operation and applications," *Proceedings of the IEEE*, vol. 90, no. 6, pp. 1022–1031, June 2002.

[9] A. Ç. Ulusoy *et al.*, "An ultra-wideband, hybrid, distributed power amplifier using flip-chip bonded GaN devices on AlN substrate," in *2014 44th European Microwave Conference*, Oct 2014, pp. 1285–1288.

[10] H. Sledzik *et al.*, "GaN based power amplifiers for broadband applications from 2 GHz to 6 GHz," in *The 40th European Microwave Conference*, Sept 2010, pp. 1658–1661.

[11] T. Maier *et al.*, "Active harmonic source-/load-pull measurements of algan/gan hemts at x-band frequencies," in *83rd ARFTG Microwave Measurement Conference*, June 2014, pp. 1–4.

[12] [Online]. Available: https://www.maurymw.com/

[13] R. Hilton and S. Dudkiewicz, "Overcoming the Challenges of On-Wafer Load Pull Measurements at Millimeter-Wave Frequencies for 5G Applications (Maury Microwave Application Note 5A-070)," *Microwave Journal*, vol. 61, no. 6, pp. 84–92, June 2018.

[14] [Online]. Available: https://www.wolfspeed.com/downloads/dl/file/id/306/product/115/cgh40006p.pdf